THE JOURNAL OF PHYSICAL CHEMISTRY B

Article

pubs.acs.org/JPCB

Probing Mercury(II)−DNA Interactions by Nanopore Stochastic Sensing

Guihua Wang,[†] Qitao Zhao,[‡] Xiaofeng Kang,[§] and Xiyun Guan*[,†]

[†]Department of Biological and Chemical Sciences, Illinois Institute of Technology, 3101 South Dearborn Street, Chicago, Illinois 60616, United States

[‡]Department of Chemistry and Biochemistry, The University of Texas at Arlington, 700 Planetarium Place, Arlington, Texas 76019-0065, United States

[§]College of Chemistry and Materials Science, Northwest University, Xian, 710069, P.R. China

Supporting Information

ABSTRACT: In this work, DNA−Hg(II) interactions were investigated by monitoring the translocation of DNA hairpins in a protein ion channel in the absence and presence of metal ions. Our experiments demonstrate that target-specific hairpin structures could be stabilized much more significantly by mercuric ions than by the stem length and the loop size of the hairpin due to the formation of Thymine−Hg(II)−Thymine complexes. In addition, the designed DNA probe allows the development of a highly sensitive nanopore sensor for Hg^{2+} with a detection limit of 25 nM. Further, the sensor is specific, and other tested metal ions including Pb^{2+}, Cu^{2+}, Cd^{2+}, and so on with concentrations of up to 2 orders of magnitude greater than that of Hg^{2+} would not interfere with the mercury detection.

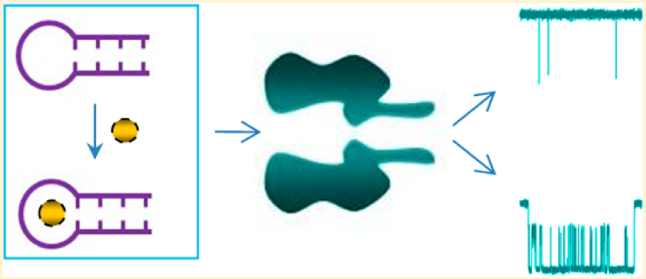

INTRODUCTION

DNA hybridization and its reverse process melting are ubiquitous in cell biology.[1−4] Given the proofreading capability of DNA polymerases, cell division stems from the unwinding of DNA helix for the reproduction of complementary strands, ensuring faithful DNA replication. Although DNA instability or damages may induce harmful mutations and cause insults to genomic integrity in this context, low fidelity DNA synthesis is beneficial for the evolution and diversity of species, as well as the development of immune systems.[5,6] Since DNA polymers are structurally polyanionic and malleable, metals are crucial for maintaining the genomic integrity and functionalities of cellular DNA during cell proliferation.[7−14] The importance of such DNA−metal interactions is 2-fold. First, physiological response to metallic stimuli is required for regulating genetic information transfer. Second, depending upon the type and the level of metal exposure,[15] gene proliferative responses caused by metal stress often involve excess gene expressions coupled with DNA conformational changes that could confer resistance to metal toxicity.[16] A better understanding of how DNA interplays with metals is therefore fundamentally important in biophysics, and would be beneficial for the design of DNA structures with conferred properties applicable in DNA-based drugs as well as molecular sensing.[17−19]

Thus far, numerous techniques have been utilized to study metal ion−DNA interactions. These include UV-absorption,[20,21] fluorescence spectroscopy,[22−26] volumetric characterization,[27] NMR,[28] X-ray crystallography,[29] and so on. Although much information regarding the effect of metal ions on the structure, conformation, and function of DNA has been obtained, more information is needed to completely understand how metal ions affect DNA folding and unfolding. In this work, we study the effect of metal ions on the stability of DNA hairpins having varying loop sizes and stem lengths by monitoring the interaction between DNA polymers and a protein ion channel in the absence and presence of metal ions. Previous studies have demonstrated that protein pores have become a valuable molecular tool to investigate biopolymers at the single-molecule level,[30,31] such as the characterization and discrimination of individual polynucleotide molecules,[32] analysis of DNA duplex formation, and the study of hairpin unzipping kinetics.[33−39]

EXPERIMENTAL SECTION

Materials and Reagents. DNA samples with standard purification (desalting), including 5′-CTAGAAAACTAG-3′, 5′-CTAGTAATCTAG-3′, 5′-CTAGTTTTCTAG-3′, 5′-CTAATG-3′, 5′-CGTAATCG-3′, 5′-CTGTAATCAG-3′, 5′-CTAGTATCTAG-3′, 5′-CTAGTAAATCTAG-3′, 5′-CTAGTTAATTCTAG-3′, 5′-CTAGTTTAATTTCTAG-3′, and so on (note that the hairpin loop regions are underlined), were purchased from Integrated DNA Technologies, Inc. (Coralville, Iowa). All the metal salts used in this work such as $Hg(NO_3)_2$ (≥99.99% trace metals basis, Product #: 516953), $Cu(NO_3)_2$

Received: September 25, 2012
Revised: April 4, 2013
Published: April 8, 2013

   dx.doi.org/10.1021/jp309541h | J. Phys. Chem. B 2013, 117, 4763−4769

(99.999% trace metals basis, Product #: 229636), $Co(NO_3)_2$ (99.999% trace metals basis, Product #: 203106), $Ni(NO_3)_2$ (99.999% trace metals basis, Product #: 203874), $Pb(NO_3)_2$ (99.999% trace metals basis, Product #: 203580), $La(NO_3)_3$ (99.999% trace metals basis, Product #: 203548), $Mg(NO_3)_2$ (99.999% trace metals basis, Product #: 203696), $Ca(NO_3)_2$ (≥99.0%, Product #: C4955), $Cd(NO_3)_2$ (99.9999% trace metals basis, Product #: 229520), $AgNO_3$ (99.999% trace metals basis, Product #: 204390), and KNO_3 (99.999% trace metals basis, Product #: 542040) were obtained from Sigma (St. Louis, MO). Both HCl (ACS reagent, ≤1 ppm heavy metals) and Trizma base (BioXtra grade, ≥99.9%) were also bought from Sigma. All of the DNA samples and chemicals were dissolved in HPLC-grade water (<1 ppm residue, ChromAR, Mallinckrodt Baker). With the exception of the stock solutions of metal salts, which were prepared at concentrations of 10 mM each, all the stock solutions of DNA polymers were prepared at 0.5 mM each, and were kept at −20 °C before and after use. The electrolyte solution used in this work contained 1 M KNO_3 and 10 mM Trizma base, with the pH of the solutions adjusted to 8.0 using hydrochloric acid. It should be noted that nitric acid should have been used for the purpose of adjusting the pH of the electrolyte solution. Adjusting pH with hydrochloric acid would introduce a trace amount of chloride ions, which might bind metal ions to decrease their effective concentrations, especially when the concentrations of metal ions are very low. Lipid 1,2-diphytanoylphosphatidylcholine was obtained from Avanti Polar Lipids (Alabaster, AL). Teflon film was purchased from Goodfellow (Malvern, PA).

Preparation and Formation of Protein Pores. The mutant αHL M113F gene was constructed by site-directed mutagenesis (Mutagenex, Piscataway, NJ) with a wild-type αHL gene in a T7 vector (pT7−αHL).[40] Wild-type αHL and mutant αHL monomers were first synthesized by coupled in vitro transcription and translation (IVTT) using the *Escherichia coli* T7 S30 Extract System for Circular DNA from Promega (Madison, WI). Subsequently, they were assembled into homoheptamers by adding rabbit red cell membranes and incubating for 1−2 h.[41] The heptamers were then purified by SDS-polyacrylamide gel electrophoresis and stored in aliquots at −80 °C.[42]

Electrical Recording. A bilayer of 1,2-diphytanoylphosphatidylcholine was formed on an aperture (150 μm) in a Teflon septum (25 μm thick) that divided a planar bilayer chamber into two compartments: *cis* and *trans*. The formation of the bilayer was achieved by using the Montal−Mueller method.[43] All the experiments were performed under a series of symmetrical buffer conditions with a 2.0 mL solution comprising 1 M KNO_3, and 10 mM Tris·HCl (pH 8.0) at 22 ± 1 °C. Unless otherwise noted, the αHL proteins, DNA polymers, and metal salts were added to the *cis* compartment, which was connected to the "ground". The final concentration of the αHL proteins used for the single channel insertion was 0.2−2.0 ng·mL^{-1}. The transmembrane potential, which was applied with Ag/AgCl electrodes with 3% agarose bridges containing 3 M KCl, was +120 mV, unless otherwise noted. A positive potential indicates a higher potential in the *trans* chamber of the apparatus. Currents were recorded with a patch clamp amplifier (Axopatch 200B, Molecular Devices; Sunnyvale, CA, USA). They were low-pass filtered with a built-in four-pole Bessel filter at 10 kHz and sampled at 50 kHz by a computer equipped with a Digidata 1322 A/D converter (Molecular Devices).

Data Analysis. Data were analyzed with the following software: pClamp 10.2 (Molecular Devices) and Origin 7.0 (Microcal, Northampton, MA). Thermodynamics of hairpin folding was obtained from the UNAFold web server.[44] Conductance values were obtained from the amplitude histograms after the peaks were fit to Gaussian functions. The values of τ_{on} (the mean interevent interval) and τ_{off} (the mean residence time) for DNA polymers and Hg(II)−DNA complexes were obtained from the dwell time histograms by fitting the distributions to single exponential functions by the Levenberg−Marquardt procedure.[45] Reaction formation constants K_f for DNA polymers or Hg(II)−DNA complexes in the protein pore were calculated by using $K_f = (\tau_{off})/(C\tau_{on})$, where C is the concentration of the DNA polymer or Hg(II)−DNA complex. It should be noted that, without Hg^{2+}, DNA samples produced only one major type of events with mean residence times of ∼100 to 300 μs. In contrast, after addition of Hg^{2+}, in addition to the rapid events, another type of long-lived events with mean residence times of milliseconds or larger appeared, most (∼95%) of which showed substate current modulations. It is apparent that these long-lived events were attributed to Hg(II)−DNA complexes. To minimize the potential interference from the uncomplexed DNA events, only the events with substate current modulations were used to calculate τ_{off} for Hg(II)−DNA complexes. These events can be well separated from others in that the amplitude of the event with substate current modulations could be obtained based on the mean value of its upper current levels. According to the literature, the reaction formation constant for the Thymine−Hg(II)−Thymine complex is on the order of 10^6 M^{-1}. Under our experimental conditions (i.e., 5 μM DNA and 5 μM Hg^{2+} throughout the entire work except dose−response and selectivity studies), ∼64% of Hg^{2+} molecules could react with the thymine-containing hairpins to form Hg^{2+}−DNA complexes. Therefore, in the calculation of the K_f values for Hg(II)−DNA complexes, 3.2 μM (= 5.0 μM × 0.64) concentrations were used. We admit that there were 5% uncertainties in these K_f values due to the inability to clearly identify all the Hg(II)−DNA complexes (5% of the long-lived events without substate current modulations were excluded in the statistical analysis of τ_{on} and τ_{off}). Each single-channel current trace was recorded for at least 2 min. At least three separate experiments were carried out for each DNA sample.

RESULTS AND DISCUSSION

Hairpins are naturally occurring and highly conserved motifs that regulate gene expressions in nucleic acids. Repetitive DNA sequence patterns, which account for about 20% of the human genome,[46] are predisposed to genomic instability,[47] leading to a series of neurological disorders as a result of the formation of hairpin-like structures.[48,49] Typically, the formation of a stem-loop structure is dependent on the base-pairings in complementary arms and mismatch arrangements in loop regions, wherein the former determines the stability of the helix, while the latter destabilizes the hairpin DNA by initiating the breakage of intramolecular bridges.

The principle for nanopore detection of metal−DNA hairpin interactions is shown in Scheme 1. Without target metal ions, the interaction between DNA and the protein pore produces only one major type of events. Once metal ions are added to the solution and incorporated into loop-forming DNA

dx.doi.org/10.1021/jp309541h | J. Phys. Chem. B 2013, 117, 4763−4769

Scheme 1. Monitoring of Metal–DNA Interaction in a Protein Ion Channel[a]

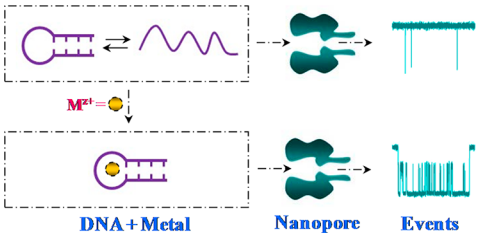

[a]The interactions of DNA and metal–DNA complexes with the pore produce events having significantly different signatures, thus permitting them to be readily differentiated.

polymers, the stable metal–DNA complexes result in events having significantly different signatures (e.g., with longer residence times and/or having substate current modulations) from those in the absence of metal ions, and hence could readily be recognized.

To demonstrate this concept, target-specific DNA hairpin probes for the recognition of mercury ions (Hg^{2+}) were designed. It is well-known that heavy metals inhibit the activity and fidelity of cellular DNA proliferation because of the formation of DNA–metal complexes, among which mercury is an extremely mutagenic element for human health.[50,51] For example, mercury bioaccumulation in such exposures as dental amalgam and flu shots may induce the production of free radicals and oxidative stress in the nervous system,[52] causing DNA instability and thus leading to chronic degenerative dementias including Alzheimer's and Parkinson's diseases.[10,16] Earlier in vitro studies have revealed that DNA hairpin-loops usually contain four mismatches.[53] To show the importance of thymine in the loop region for recognition of mercuric ions, three tetraloop DNA molecules with the sequence of 5′-CTAGTTTTCTAG-3′ (4T), 5′-CTAGTAATCTAG-3′ (2T), and 5′-CTAGAAAACTAG-3′ (0T) were examined (note that the loop regions are underlined). Since the closed state of a hairpin has a larger diameter than the constriction of the wild-type α-hemolysin pore, in order to translocate such a DNA molecule through this pore, the hairpin must be unfolded, thus resulting in a significantly longer residence time event than the open state of the hairpin (i.e., a single-stranded DNA molecule).[54] To facilitate discriminating metal–DNA complex events against the mixed (closed state and open state) hairpin events, an engineered α-hemolysin protein $(M113F)_7$ pore was used since rapid unzipping of double-stranded DNA[55] and DNA hairpins (Figure 1) in this pore could be obtained. Further, the commonly used NaCl or KCl solution in nanopore stochastic sensing was replaced with KNO_3 to prevent possible interactions between Cl^- and some heavy metal ions such as Hg^{2+} and Pb^{2+}.

Our single-channel recording experiments showed that, in the absence of Hg^{2+}, all three DNA samples produced only one major type of events with a mean residence time of ~170 μs at an applied potential bias of +120 mV (Figure 1). According to UNAFold calculation,[44] all three of these DNA polymers could form thermodynamically stable hairpin structures (Supporting Information, Table S1). The results suggest that the closed state of the hairpin was unfolded immediately in our experimental conditions (i.e., with the combination of the $(M113F)_7$ pore and the KNO_3 electrolyte solution) so that it was driven through the pore with the residence time similar to

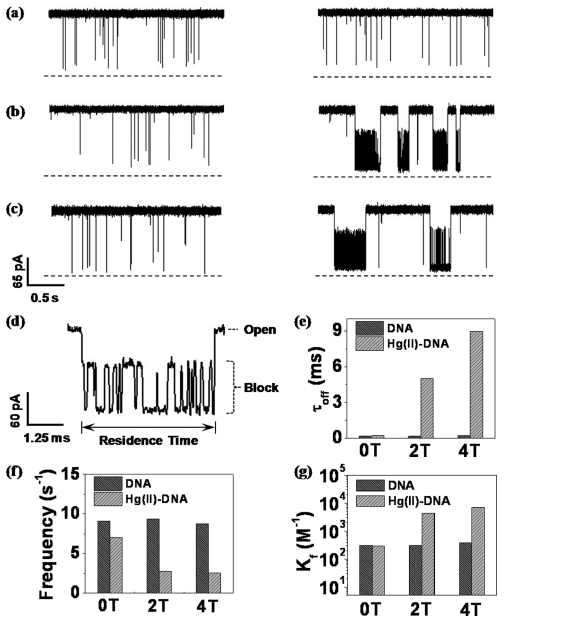

Figure 1. The effect of loop sequence on the Hg(II)–DNA hairpin interaction. Representative single-channel recordings of (a) 5′-CTAGAAAACTAG-3′, (b) 5′-CTAGTAATCTAG-3′, and (c) 5′-CTAGTTTTCTAG-3′ in the (left) absence and (right) presence of Hg^{2+}. (d) A typical long-lived event containing substate current modulations shown at an expanded time scale and plots of (e) event mean residence time, (f) event frequency, and (g) reaction formation constant vs DNA hairpins having different loop sequences. Dashed lines represent the levels of zero current. The experiments were performed at +120 mV in the presence of 5 μM DNA samples. The concentration of added Hg^{2+} was 5 μM.

that of the open state of the hairpin. After addition of mercuric ions to the solution, events with significantly different signatures were observed with the 4T and 2T DNA polymers, while the event mean residence time and frequency as well as the overall reaction formation constant K_f for the 0T DNA sample in the nanopore did not change much (Figure 1, and Supporting Information, Figure S1). Specifically, compared with the events in the absence of Hg^{2+}, in the presence of mercuric ions, the event residence times of the 2T and 4T DNA samples increased ~30- and ~40-fold, respectively, while the event frequency of both these two DNA samples decreased ~3-fold (note that presence of Hg^{2+} in the solution would not lead to channel gating). Thus, the overall reaction formation constants K_f for 2T and 4T DNA samples in the nanopore increased ~9- and ~12-fold, respectively. The results suggest that these two DNA polymers could interact with Hg^{2+} and form stable Thymine–Hg(II)–Thymine complexes.[56,57] The reason why the DNA–Hg(II) complex events were much less frequent than those of uncomplexed DNA samples may be due to the decrease in the net negative charge of the polymers. Furthermore, we noticed that these long-lived Thymine–Hg(II)–Thymine complex events showed substate current modulations, suggesting that these events may be attributed to the translocation of the Hg^{2+}–DNA hairpin complexes through the pore after unzipping.[55] This interpretation is supported by the voltage dependence experiment, where the mean residence time of the long-lived events decreased as the applied potential bias increased (Supporting Information, Figure S2). In addition, the 4T DNA molecule produced events with a larger mean residence time than those of 2T (9.0 ms vs 5.0 ms), as a

dx.doi.org/10.1021/jp309541h | J. Phys. Chem. B 2013, 117, 4763–4769

result of a smaller hairpin loop closing barrier (δ_{4T} = 1.68 kcal·mol^{-1}, δ_{2T} = 2.18 kcal·mol^{-1}, see Supporting Information, Table S1).

The effect of Hg^{2+} on DNA hairpins with varying stem lengths but having the same loop sequence was then investigated. The DNA polymers examined included CTAATG, CGTAATCG, CTGTAATCAG, and CTAGTAATCTAG (note that the loop regions are underlined). Our experiments showed that when DNA had a short hairpin stem region, e.g., less than three base pairs, only one major type of short-lived events was produced; further, the event mean residence time and frequency as well as the overall reaction formation constant did not change significantly in the absence and presence of mercury ions. However, in sharp contrast, when the hairpin had a stem of at least three base pairs, after addition of Hg^{2+} to the hairpin solution, in addition to the rapid events, another type of long-lived events (with the mean residence time ~25 folds longer than those of short-lived ones) appeared. Similar to the observation made with the 2T and 4T DNA samples, these long-lived events were ~3 folds less frequent than those short-lived ones observed in the absence of Hg^{2+}; further, many of these long-lived events had intermediate current blockage levels, suggesting the formation of stable Hg(II)−hairpin complexes (Figure 2 and Supporting Information, Figure S3). As an important aside, we noticed that, in the absence of Hg^{2+}, although the event mean residence time did not change significantly for the four tested DNA samples, the event frequencies of CTAAAG and CGTAATCG were ~10 folds larger than those of CTGTAATCAG and CTAGTAATCTAG.

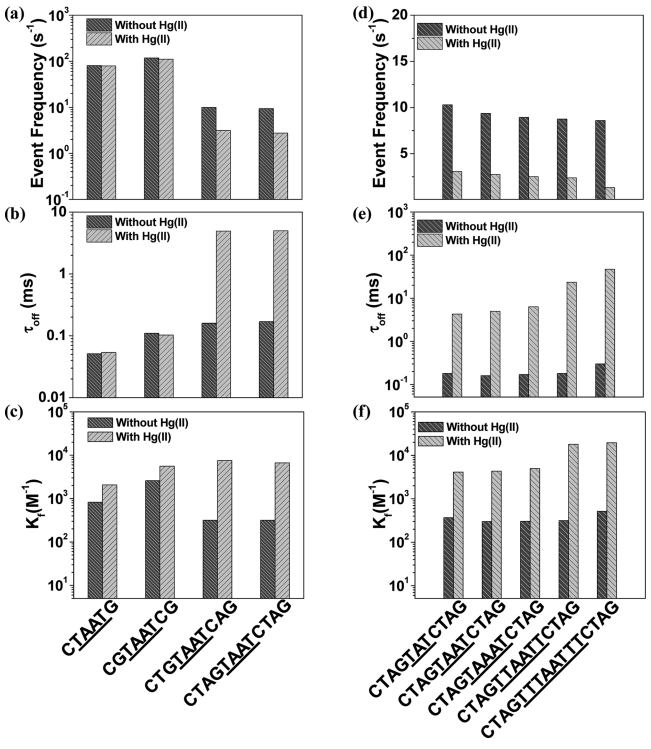

Figure 2. Effect of the hairpin stem length on the (a) event frequency, (b) residence time, and (c) reaction formation constant of Hg(II)−DNA complexes, and effect of the hairpin loop size on the (d) event frequency, (e) residence time, and (f) reaction formation constant of Hg(II)−DNA complexes. The experiments were performed at +120 mV in the presence of 5 μM DNA samples. The concentration of added Hg^{2+} was 5 μM.

This suggests that the structures/conformations of CTAAAG and CGTAATCG were different from those of the other two DNA samples. The UNAFold calculation showed that with the exception of CTAAAG, all the other three DNA samples could form thermodynamically stable hairpin structures (the T_m values of CGTAATCG, CTGTAATCAG, and CTAGTAATCTAG were 29.2 °C, 38.9 °C, and 42.9 °C, respectively). One likely reason why CTAAAG and CGTAATCG showed similar behaviors in our experiments is that CGTAATCG existed predominantly in the open state form in our nanopore experimental conditions. Taken together, although Hg^{2+} affected the stability of the target-specific hairpin structure much more significantly than the hairpin stem length did (note that, in the absence of Hg^{2+}, the mean residence time of the DNA events only increased by ~2 folds as the stem length increased from 2 base pairs to 4 base pairs, while after addition of Hg^{2+} to the solution, the event mean residence time and the overall reaction formation constant for the DNA hairpin CTGTAATCAG or CTAGTAATCTAG in the α-hemolysin pore increased by ~25-fold and ~7-fold, respectively), our results demonstrated that in order to observe such a metal ion effect, the DNA polymer should first be able to form a stable hairpin structure so that Hg^{2+} could be incorporated into the hairpin loop and form a stable Thymine−Hg(II)−Thymine complex.

To further elucidate the influence of mercuric ions on the stability of hairpin DNA molecules, hairpins with identical stems but varying loop sizes (some of which had different loop sequences) were examined. Our experimental results (Figure 2 and Supporting Information, Figure S4) showed that, in the absence of Hg^{2+}, the event frequency decreased by ~16%, while the event mean residence time increased by ~67% as the hairpin loop length increased from 3 bases to 8 bases. In contrast, in the presence of Hg^{2+}, with an increase in the hairpin loop length from 3 bases to 8 bases, the event frequency decreased by ~120%, while the event residence time increased by ~11-fold. It is worth mentioning that regarding the two DNA samples (CTAGTATCTAG and CTAGTAAATCTAG), the event residence time increased by 47% when two additional adenines were introduced into the loop of the DNA hairpin, while a 9.4-fold increase in the event residence time was observed with CTAGTAATCTAG and CTAGTTTAATTTCTAG, where four additional thymines were introduced in the loop. The results again demonstrated the importance of thymine in the loop region for recognition of mercuric ions. The sharp increase in the event residence time of CTAGTTTAATTTCTAG over CTAGTAATCTAG may be due to the simultaneous binding of two or more Hg^{2+} ions to CTAGTTTAATTTCTAG, thus forming a more stable Hg(II)−DNA complex. Furthermore, similar to the observation made with hairpins with different stem lengths, after addition of Hg^{2+}, all five of the DNA hairpin samples produced events with 3-fold smaller frequency but having ~25-fold or larger residence time and at least 7-fold greater reaction formation constant in the nanopore than those without Hg^{2+}. It is apparent that coordination of metal ions with DNA loops results in the formation of more stable hairpin structures.

Taken together, the combined results demonstrated that Hg^{2+} could affect the stability of the target-specific hairpin structure much more significantly than the stem length and loop size did due to the formation of stable metal−DNA complexes.

dx.doi.org/10.1021/jp309541h | J. Phys. Chem. B 2013, 117, 4763−4769

Since the addition of Hg^{2+} to the DNA solution could result in events having significantly different signatures (e.g., with longer residence times and having substate current modulations) from those in the absence of metal ions with a properly engineered nanopore, metal-stabilized DNA offers the potential to develop highly sensitive sensors for Hg^{2+}. To demonstrate the proof-of-concept of this sensor application, the interaction between the hairpin DNA with the sequence of 5′-CTAG-TAATCTAG-3′ (note that the loop region is underlined) and various concentrations of mercury ion was examined. As shown in Figures 3 and 4a, with an increase in the concentration of added Hg^{2+}, the frequency of DNA−Hg(II) complex events increased. The detection limit (defined as the concentration corresponding to 3 times the standard deviation of a blank signal) for the detection of Hg^{2+} with this sensing system is 25 nM. Such a detection limit can be achieved in a ∼1 min single-channel recording. To test the selectivity of this nanopore sensor, a series of other metal ions was examined, including Pb^{2+}, Cd^{2+}, Cr^{3+}, Zn^{2+}, Co^{2+}, etc. It is known that these metal ions, especially Pb^{2+}, are able to interact with thymines, thus interfering with the Hg^{2+} detection.[57,58] Previous studies have also demonstrated that the interferences from these metal ions could be eliminated by addition of 2,6-pyridinedicarboxylic acid (PDCA) since PDCA can strongly complex with other metal ions but would not significantly affect the interaction between Hg^{2+} and thymines. Our single-channel recording experiments (Figure 4b) showed that, even without PDCA, the characteristic long duration events of the Hg(II)−thymine complexes were rarely observed with the DNA hairpin CTAGTAAT-CTAG in the presence of other metal ions (∼1 event per 100 s at metal ion concentrations of 5 μM). In contrast, the same concentration of Hg^{2+} produced ∼230 events in 100 s. The comparison results suggest that this sensor is highly selective to Hg^{2+}.

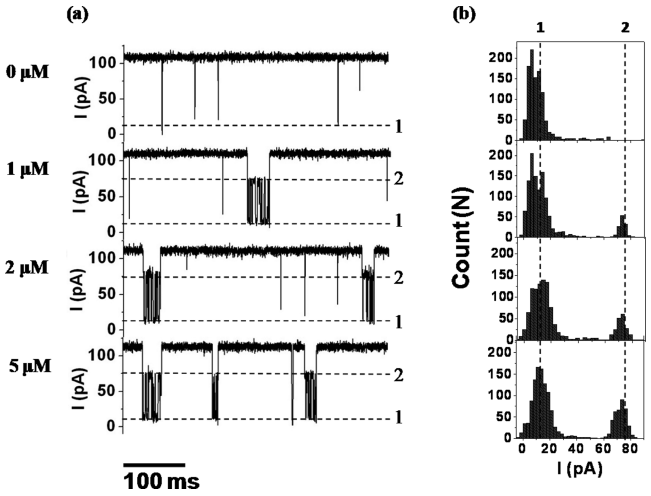

Figure 3. Nanopore detection of Hg^{2+}. (a) Representative single channel recordings of 5 μM DNA (sequence: 5′-CTAGTAATCTAG-3′) in the presence of mercuric ions at various concentrations. (b) The corresponding concentration-dependent event amplitude histograms. To facilitate the separation of the events having substate current modulations from others, the amplitude of the event with substate current modulations was obtained based on the mean value of its upper current levels. Dashed line 1 represents the blockage events attributed to free DNA polymers and DNA−metal complexes, which would not cause substate current modulations, while dashed line 2 represents the events due to the DNA−metal complexes producing substate current modulations. The experiments were performed at +120 mV.

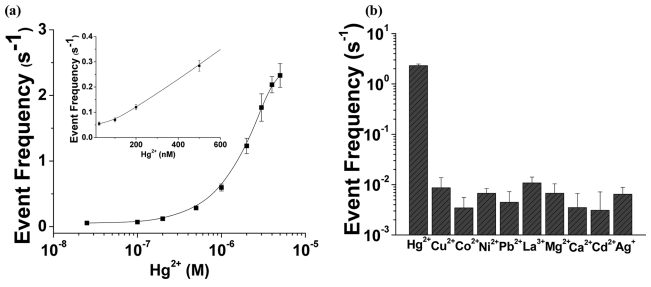

Figure 4. (a) Dose−response curve and (b) selectivity for the mercury ion nanopore sensor system. The inset of panel a shows an enlarged portion of the dose−response curve at a range of low Hg^{2+} concentrations. The experiments were performed at +120 mV in the presence of 5 μM DNA with a sequence of 5′-CTAGTAATCTAG-3′. Only the long-lived events having substate current modulations were included in the analysis of the event frequency (f). Note that the event frequency with 25 nM Hg^{2+} was estimated by dividing the number of events by the recording time since the number of events (∼30 events) collected in a 10 min recording was not enough for accurate statistical analysis.

It should be mentioned that this sensing system is not optimized. Our experimental results (Figures 1 and 2) demonstrated that, with an increase in the loop size of the hairpin and especially if the loop contains more thymines, the event residence time and the reaction formation constant increased, suggesting the formation of more stable DNA−Hg^{2+} complexes. Thus, using DNA hairpins with longer loop regions or having more thymines in the loop might potentially help to improve the sensor sensitivity. However, one major issue using these DNA hairpins is that the event frequency decreased with an increase in the loop size or in the number of thymines. To develop a rapid sensor, a larger event frequency is desired. Therefore, using hairpins with small loops may be useful to lower the detection limit of the sensor. Recently, Wen et al. employed the same DNA−metal interaction approach to develop a highly sensitive and selective nanopore sensor for mercuric ion.[59] Unlike our sensor design, where the hairpin loop contained the binding site for Hg^{2+}, the mercury binding site of their sensor was located in the stem region of the hairpin. Using a similar symmetric electrolyte condition, their approach could detect Hg^{2+} as low as ∼0.7 μM. In addition to the different DNA probes, the lower detection limit of our sensor is likely due to the different αHL nanopores used (i.e., the engineered $(M113F)_7$ vs the wild-type). Furthermore, in our study, only the long-lived events with substate current modulations were counted as the events produced by the Hg^{2+}-DNA complexes so that an extremely low background could be obtained. By employing an asymmetric electrolyte gradient instead of the symmetric electrolyte condition, Wen et al. successfully lowered the detection limit of their sensor to ∼7 nM. This asymmetric electrolyte gradient strategy may also work in our system to improve the sensor sensitivity. In addition, the detection limit of the sensor may potentially be lowered by adjusting other experimental conditions such as the pH value of the buffer solution,[60] the concentration of the DNA hairpin, and so on.

■ CONCLUSIONS

The effect of metal ions on the stability of DNA hairpins was investigated by using nanopore technology. Our experimental

dx.doi.org/10.1021/jp309541h | J. Phys. Chem. B 2013, 117, 4763−4769

results provided evidence that the interaction between mercury and thymine led to the formation of a bridged complex T–Hg(II)–T, which could stabilize the hairpin structure much more significantly than the stem length and loop size of the hairpin did. Given the significantly different responses of the designed DNA probe to different metal ions, a highly sensitive and selective nanopore sensor for the detection of Hg^{2+} was successfully developed based on the formation of stable T–Hg(II)–T complexes. This coordination chemistry approach should find useful application in the development of nanopore sensors for other metal ions.

■ ASSOCIATED CONTENT

Supporting Information

Additional table and figures. This material is available free of charge via the Internet at http://pubs.acs.org.

■ AUTHOR INFORMATION

Corresponding Author

*Mailing address: Department of Biological and Chemical Sciences, Illinois Institute of Technology, 3101 S. Dearborn St., Chicago, IL 60616, USA. Tel: 312-567-8922; Fax: 312-567-3494. E-mail: xguan5@iit.edu.

Notes

The authors declare no competing financial interest.

■ ACKNOWLEDGMENTS

This work was financially supported by the Defense Advanced Research Projects Agency (HR0011-10-C-0226), the National Institutes of Health (1R011HG005095), Department of Homeland Security (HSHQDC-09-C-00091), and the National Natural Science Foundation of China (21175105).

■ REFERENCES

(1) Weaver, D. T.; DePamphilis, M. L. The Role of Palindromic and Non-palindromic Sequences in Arresting DNA Synthesis *in Vitro* and *in Vivo*. *J. Mol. Biol.* **1984**, *180*, 961–986.

(2) Ma, H.; Wan, C.; Wu, A.; Zewail, A. H. DNA Folding and Melting Observed in Real Time Redefine the Energy Landscape. *Proc. Natl. Acad. Sci. U.S.A.* **2007**, *104*, 712–716.

(3) Dai, X.; Greizerstein, M. B.; Nadas-Chinni, K.; Rothman-Denes, L. B. Supercoil-Induced Extrusion of a Regulatory DNA Hairpin. *Proc. Natl. Acad. Sci. U.S.A.* **1997**, *94*, 2174–2179.

(4) Schoen, I.; Krammer, H.; Braun, D. Hybridization Kinetics is Different inside Cells. *Proc. Natl. Acad. Sci. U.S.A.* **2009**, *106*, 21649–21654.

(5) Makovets, S.; Blackburn, E. H. DNA Damage Signaling Prevents Deleterious Telomere Addition at DNA Breaks. *Nat. Cell Biol.* **2009**, *11*, 1383–1386.

(6) Mandal, P. K.; Blanpain, C.; Rossi, D. J. DNA Damage Response in Adult Stem Cells: Pathways and Consequences. *Nat. Rev. Mol. Cell Biol.* **2011**, *12*, 198–202.

(7) Tullius, T. D. Metals and Molecular Biology. In *Metal–DNA Chemistry*; Tullius, T. D., Ed.; ACS Symposium Series; American Chemical Society: Washington, DC, 1989; Vol. *402*, Chapter 1, pp 1–23.

(8) Dubyak, G. R. Ion Homeostasis, Channels, and Transporters: An Update on Cellular Mechanisms. *Adv. Physiol. Educ.* **2007**, *28*, 143–154.

(9) Müller, J. Functional Metal Ions in Nucleic Acids. *Metallomics* **2010**, *2*, 318–327.

(10) Rönnbäck, L.; Hansson, E. Chronic Encephalopathies Induced by Mercury or Lead: Aspects of Underlying Cellular and Molecular Mechanisms. *Br. J. Ind. Med.* **1992**, *49*, 233–240.

(11) Gray, H. B. Biological Inorganic Chemistry at the Beginning of the 21st Century. *Proc. Natl. Acad. Sci. U.S.A.* **2003**, *100*, 3563–3568.

(12) Ma, H.; Wan, C.; Zewail, A. H. Dynamics of Ligand Substitution in Labile Cobalt Complexes Resolved by Ultrafast T-Jump. *Proc. Natl. Acad. Sci. U.S.A.* **2008**, *105*, 12754–12757.

(13) Lippard, S. J. The Inorganic Side of Chemical Biology. *Nat. Chem. Biol.* **2006**, *2*, 504–507.

(14) Hud, N. V. *Nucleic Acid–Metal Ion Interactions*; Royal Society of Chemistry: Cambridge, UK, 2009; pp75–112.

(15) Predki, P. F.; Sarkars, B. Effect of Replacement of "Zinc Finger" Zinc on Estrogen Receptor DNA Interactions. *J. Biol. Chem.* **1992**, *267*, 5842–5846.

(16) Palmiter, R. D. The Elusive Function of Metallothioneins. *Proc. Natl. Acad. Sci. U.S.A.* **1998**, *95*, 8428–8430.

(17) Rothemund, P. W. K. Folding DNA to Create Nanoscale Shapes and Patterns. *Nature* **2006**, *440*, 297–302.

(18) Kalek, M.; Andreas, S. M.; Wengel, J. Effective Modulation of DNA Duplex Stability by Reversible Transition Metal Complex Formation in the Minor Groove. *J. Am. Chem. Soc.* **2007**, *129*, 9392–9400.

(19) Tanaka, K.; Tengeiji, A.; Kato, T.; Toyama, N.; Shionoya, M. A Discrete Self-Assembled Metal Array in Artificial DNA. *Science* **2003**, *299*, 1212–1213.

(20) Kwon, Y.; Lee, C. H.; Choi, D.; Jin, J. Materials Science of DNA. *J. Mater. Chem.* **2009**, *19*, 1353–1380.

(21) Liu, Z.; Tan, C.; Guo, X.; Kao, Y.-T.; Li, J.; Wang, L.; Sancar, A.; Zhong, D. Dynamics and Mechanism of Cyclobutane Pyrimidine Dimer Repair by DNA Photolyase. *Proc. Natl. Acad. Sci. U.S.A.* **2011**, DOI: 10.1073/pnas.1110927108.

(22) Kim, J.; Doose, S.; Neuweiler, H.; Sauer, M. The Initial Step of DNA Hairpin Folding: A Kinetic Analysis Using Fluorescence Correlation Spectroscopy. *Nucleic Acids Res.* **2006**, *34*, 2516–2527.

(23) Orden, A. V.; Jung, J. Review Fluorescence Correlation Spectroscopy for Probing the Kinetics and Mechanisms of DNA Hairpin Formation. *Biopolymers* **2007**, *89*, 1–16.

(24) Wagenknecht, H. Fluorescent DNA Base Modifications and Substitutes: Multiple Fluorophore Labeling and the DETEQ Concept. *Ann. N.Y. Acad. Sci.* **2008**, *1130*, 122–130.

(25) Hud, N. V. *Nucleic Acid-Metal Ion Interactions*; Royal Society of Chemistry: Cambridge, UK, 2009; pp 154–175.

(26) Bustamante, C. Direct Observation and Manipulation of Single DNA Molecules Using Fluorescence Microscopy. *Annu. Rev. Biophys. Biophys. Chem.* **1991**, *20*, 415–446.

(27) Fan, H. Y.; Shek, Y. L.; Amiri, A.; Dubins, D. N.; Heerklotz, H.; Macgregor, R. B., Jr.; Chalikian, T. V. Volumetric Characterization of Sodium-Induced G-Quadruplex Formation. *J. Am. Chem. Soc.* **2011**, *133*, 4518–4526.

(28) Mao, X.; Gmeiner, W. H. NMR Study of the Folding–Unfolding Mechanism for the Thrombin-Binding DNA Aptamer d(GGTTGGTGTGGTTGG). *Biophys. Chem.* **2005**, *113*, 155–160.

(29) Schmeing, T. M.; Ramakrishnan, V. What Recent Ribosome Structures Have Revealed about the Mechanism of Translation. *Nature* **2009**, *461*, 1234–1242.

(30) Derrington, I. M.; Butler, T. Z.; Collins, M. D.; Manrao, E.; Pavlenok, M.; Niederweis, M.; Gundlach, J. H. Nanopore DNA Sequencing with MspA. *Proc. Natl. Acad. Sci. U.S.A.* **2010**, *107*, 16060–16065.

(31) Venkatesan, B. M.; Bashir, R. Nanopore Sensors for Nucleic Acid Analysis. *Nat. Nanotechnol.* **2012**, *7*, 615–624.

(32) Kasianowicz, J. J.; Brandin, E.; Branton, D.; Deamer, D. W. Characterization of Individual Polynucleotide Molecules Using a Membrane Channel. *Proc. Natl. Acad. Sci. U.S.A.* **1996**, *93*, 13770–13773.

(33) Sutherland, T. C.; Dinsmore, M. J.; Kraatz, H.-B.; Lee, J. S. An Analysis of Mismatched Duplex DNA Unzipping through a Bacterial Nanopore. *Biochem. Cell Biol.* **2004**, *82*, 407–412.

(34) Howorka, S.; Cheley, S.; Bayley, H. Sequence-Specific Detection of Individual DNA Strands Using Engineered Nanopores. *Nat. Biotechnol.* **2001**, *19*, 636–639.

(35) Howorka, S.; Siwy, Z. Nanopore Analytics: Sensing of Single Molecules. *Chem. Soc. Rev.* **2009**, *38*, 2360−84.
(36) Deamer, D. Nanopore Analysis of Nucleic Acids Bound to Exonucleases and Polymerases. *Annu. Rev. Biophys.* **2010**, *39*, 79−90.
(37) Jetha, N. N.; Wiggin, M.; Marziali, A. Forming an α-Hemolysin Nanopore for Single-Molecule Analysis. *Methods Mol. Biol.* **2009**, *544*, 113−27.
(38) Healy, K. Nanopore-Based Single-Molecule DNA Analysis. *Nanomedicine* **2007**, *2*, 459−81.
(39) Efcavitch, J. W.; Thompson, J. F. Single-Molecule DNA Analysis. *Annu. Rev. Anal. Chem.* **2010**, *3*, 109−28.
(40) Song, L. Z.; Hobaugh, M. R.; Shustak, C.; Cheley, S.; Bayley, H.; Gouaux, J. E. Structure of Staphylococcal α-Hemolysin, a Heptameric Transmembrane Pore. *Science* **1996**, *274*, 1859.
(41) Cheley, S.; Braha, O.; Lu, X.; Conlan, S.; Bayley, H. A Functional Protein Pore with a "Retro" Transmembrane Domain. *Protein Sci.* **1999**, *8*, 1257.
(42) Andrews, P. Estimation of Molecular Size and Molecular Weights of Biological Compounds by Gel Filtration. *Methods Biochem. Anal.* **1970**, *18*, 1−53.
(43) Montal, M.; Mueller, P. Formation of Bimolecular Membranes from Lipid Monolayers and a Study of Their Electrical Properties. *Proc. Natl. Acad. Sci. U.S.A.* **1972**, *69*, 3561−3566.
(44) Zuker, M. Mfold Web Server for Nucleic Acid Folding and Hybridization Prediction. *Nucleic Acids Res.* **2003**, *31*, 3406−3415.
(45) Movileanu, L.; Schmittschmitt, J. P.; Scholtz, J. M.; Bayley, H. Interactions of Peptides with a Protein Pore. *Biophys. J.* **2005**, *89*, 1030−1045.
(46) Stalling, R. L.; Torney, D. C.; Hildebrand, C. E.; Longmire, J. L.; Deaven, L. L.; Jett, J. H.; Doggett, N. A.; Moyzis, R. K. Physical Mapping of Human Chromosomes by Repetitive Sequence Fingerprinting. *Proc. Natl. Acad. Sci. U.S.A.* **1990**, *87*, 6128−6222.
(47) Lin, C. T.; Lin, W. H.; Lyu, Y. L.; Whang-Peng, J. Inverted Repeats as Genetic Elements for Promoting DNA Inverted Duplication: Implications in Gene Amplification. *Nucleic Acids Res.* **2001**, *29*, 3529−3538.
(48) Liu, G.; Chen, X.; Bissler, J. J.; RSinden, R.; Leffak, M. Replication-Dependent Instability at (CTG)·(CAG) Repeat Hairpins in Human Cells. *Nat. Chem. Biol.* **2010**, *6*, 652−659.
(49) Voineagu, I.; Narayanan, V.; Lobachev, K. S.; Mirkin, S. M. Replication Stalling at Unstable Inverted Repeats: Interplay between DNA Hairpins and Fork Stabilizing Proteins. *Proc. Natl. Acad. Sci. U.S.A.* **2008**, *105*, 9936−9941.
(50) Pendergrass, J. C.; Haley, B. E.; Vimy, M. J.; Winfield, S. A.; Lorscheider, F. L. Mercury Vapor Inhalation Inhibits Binding of GTP to Tubulin in Rat Brain: Similarity to a Molecular Lesion in Alzheimer Diseased Brain. *Neurotoxicology* **1997**, *18*, 315−324.
(51) Crespo-López, M. E.; Macêdo, G. L.; Pereira, S. I.; Arrifano, G. P.; Picanço-Diniz, D. L.; do Nascimento, J. L.; Herculano, A. M. Mercury and Human Genotoxicity: Critical Considerations and Possible Molecular Mechanisms. *Pharmacol. Res.* **2009**, *60*, 212−220.
(52) Kingman, A.; Albertini, T.; Brown, L. J. Mercury Concentrations in Urine and Whole Blood Associated with Amalgam Exposure in a US Military Population. *J. Dent. Res.* **1998**, *77*, 461−71.
(53) Davison, A.; Leach, D. R. F. Two-Base DNA Hairpin-Loop Structures in Vivo. *Nucleic Acids Res.* **1994**, *22*, 4361−4363.
(54) Vercoutere, W.; Winters-Hilt, S.; Olsen, H.; Deamer, D.; Haussler, D.; Akeson, M. Rapid Discrimination among Individual DNA Hairpin Molecules at Single-Nucleotide Resolution Using an Ion Channel. *Nat. Biotechnol.* **2001**, *19*, 248−52.
(55) Liu, A.; Zhao, Q.; Krishantha, D. M.; Guan, X. Unzipping of Double-Stranded DNA in Engineered α-Hemolysin Pores. *J. Phys. Chem. Lett.* **2011**, *12*, 1372−1376.
(56) Kuklenyik, Z.; Marzilli, L. G. Mercury(II) Site-Selective Binding to a DNA Hairpin. Relationship of Sequence-Dependent Intra- and Interstrand Cross-Linking to the Hairpin−Duplex Conformational Transition. *Inorg. Chem.* **1996**, *35*, 5654−5662.
(57) Li, T.; Dong, S.; Wang, E. Label-Free Colorimetric Detection of Aqueous Mercury Ion (Hg^{2+}) Using Hg^{2+}-Modulated G-Quadruplex-Based DNAzymes. *Anal. Chem.* **2009**, *81*, 2144−2149.
(58) Li, D.; Wieckowska, A.; Willner, I. Optical Analysis of Hg^{2+} Ions by Oligonucleotide−Gold-Nanoparticle Hybrids and DNA-Based Machines. *Angew. Chem., Int. Ed. Engl.* **2008**, *47*, 3927−3931.
(59) Wen, S.; Zeng, T.; Liu, L.; Zhao, K.; Zhao, Y.; Liu, X.; Wu, H. C. Highly Sensitive and Selective DNA-Based Detection of Mercury(II) with α-Hemolysin Nanopore. *J. Am. Chem. Soc.* **2011**, *133*, 18312−18317.
(60) de Zoysa, R. S.; Krishantha, D. M.; Zhao, Q.; Gupta, J.; Guan, X. Translocation of Single-Stranded DNA through the α-Hemolysin Protein Nanopore in Acidic Solutions. *Electrophoresis* **2011**, *32*, 3034−3041.